Electroactive Biofilm-based Constructed Wetland (EABB-CW): a mesocosm-scale test of an innovative setup for wastewater treatment

Carlos A. Ramírez-Vargas[ab*], Carlos A. Arias [ab*], Pedro Carvalho[ab], Liang Zhang[ab], Abraham Esteve-Núñez[c], Hans Brix[ab]

[a]Department of Bioscience – Aquatic Biology, Aarhus University, Denmark

[b]WATEC, Aarhus University, 8000 Aarhus C, Denmark

[c]Department of Chemical Engineering – Universidad de Alcalá, Spain

*Corresponding authors

Abstract

Constructed wetlands (CWs) performance enhancement can be done with intensification strategies. A recent strategy still in study is the coupling with Microbial Electrochemical Technologies (MET). An alternative system using electro-conductive biofilters instead of electrodes and circuits used in MET, resulted in the development of a Microbial Electrochemical-based CW (METland). This system relies on electroactive bacteria (EAB) metabolism to transfer electrons to an electro-conductive material, thus boosting substrate consumption, and diminishing electron availability for biomass build-up and methane generation. In previous studies this biofilters have shown an improvement in biodegradation rates in comparison with subsurface flow CW. However, this set-up is still in development, hence there are uncertainties regarding the dynamics involve in the removal of pollutants. Considering that, this work aimed at establishing the capacity and removal kinetics of organic matter and nutrients in an

Electroactive Biofilm-Based CW (EABB-CW). Two electro-conductive materials were tested (PK-A and PK-LSN) in planted and non-planted mesocosms and compared with sand. The systems were operated in a continuous upflow mode for 32 weeks and fed with real wastewater. The electro-conductive systems reached removal efficiencies up to 88% for BOD_5, 90% for COD, 46% for NH_4-N, and 86% for PO_4-P. Organic matter removal in electro-conductive systems was possible even at loading rates 10-fold higher than recommended for horizontal flow CWs. First-order area-based removal constants (*k*), calculated for organic matter and nutrients are higher than values typically reported for saturated CW and in certain cases comparable with vertical flow CW. The organic removal was correlated with electron current densities measures, as indicator of the presence of EAB. The tested EABB-CW profiles as a promising CW type for the removal of organic matter and PO_4-P with margin for modifications to improve nitrogen removal. Future studies with pilot/real scale systems are proposed to validate the findings of this study.

Keywords

bioelectrochemical snorkel, electroactive bacteria, microbial electrochemical technology, removal kinetics, treatment wetlands.

Corresponding authors:

Carlos A. Ramírez-Vargas (e-mail: c.a.ramirez@bios.au.dk); Carlos A. Arias (e-mail: carlos.arias@bios.au.dk).

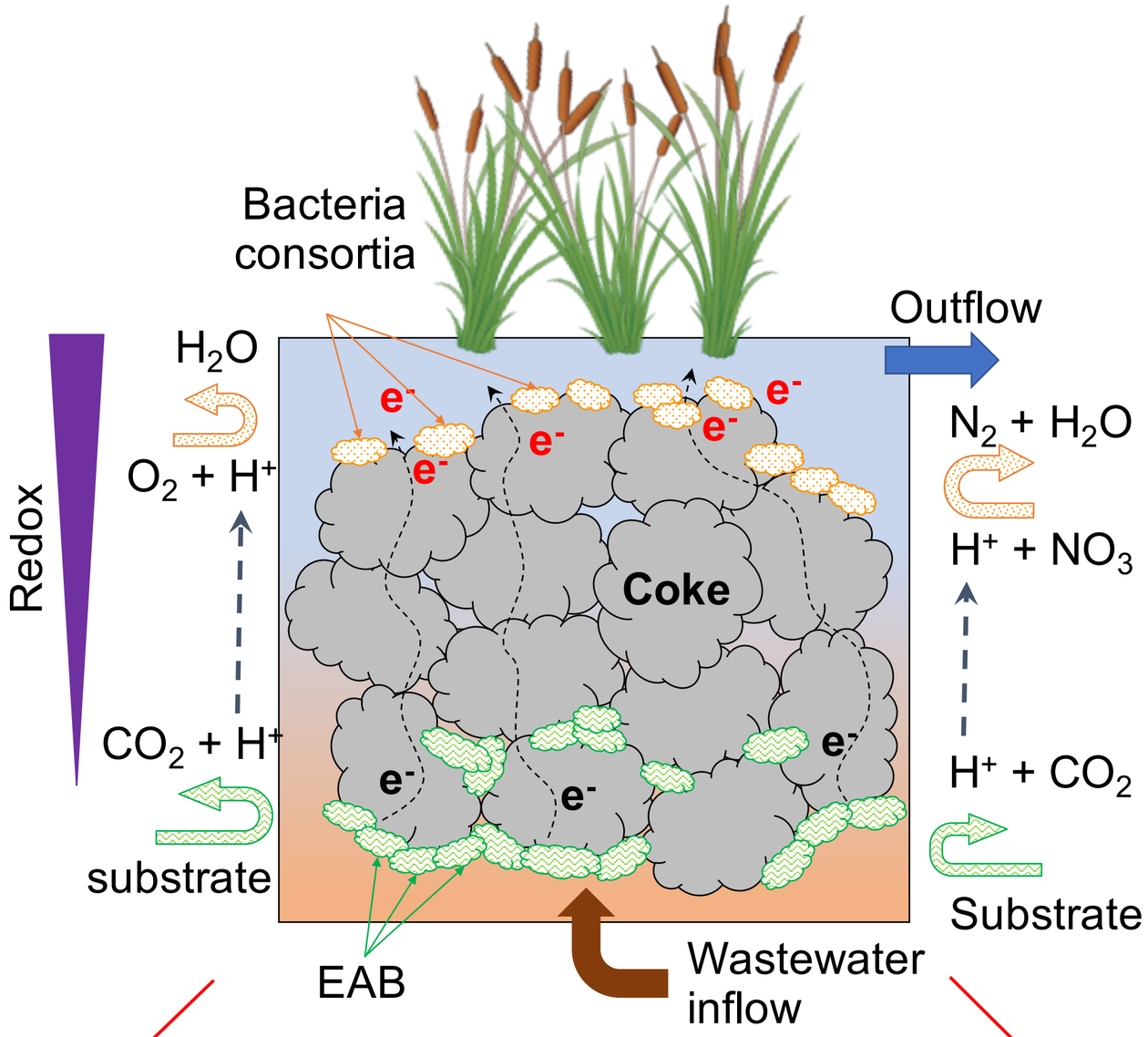

- PK-A > PK-LSN > Sand
- planted = non-planted

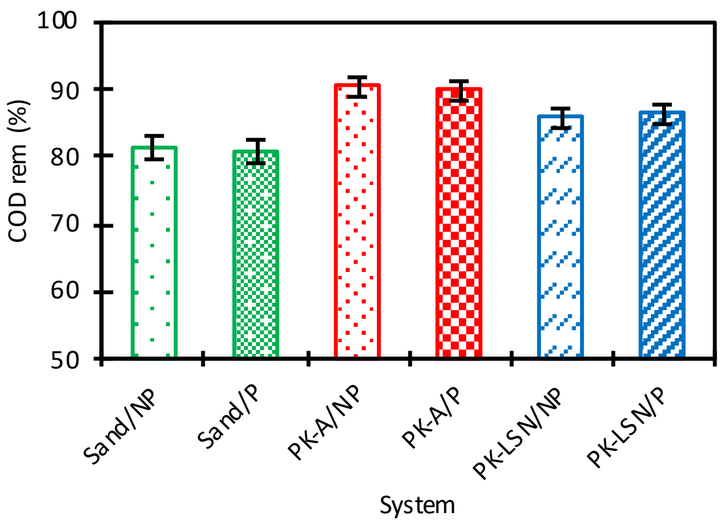

- PK-A = PK-LSN = Sand
- planted > non-

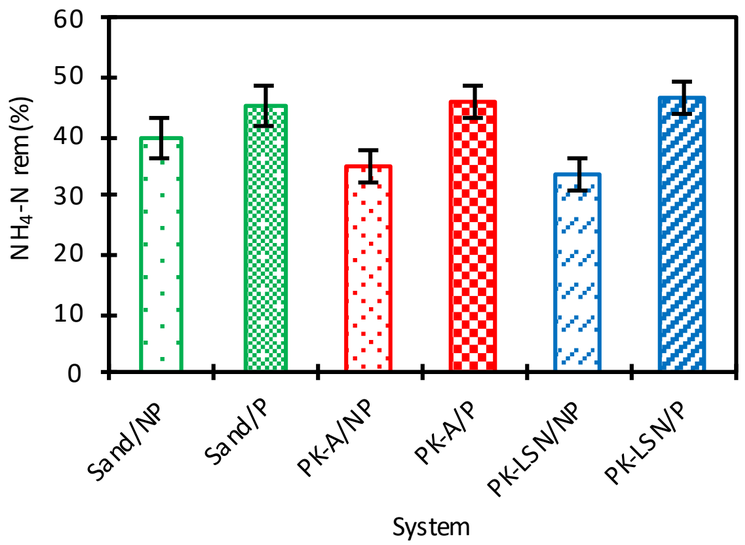

- PK-A > Coarse > Sand
- planted > non-planted

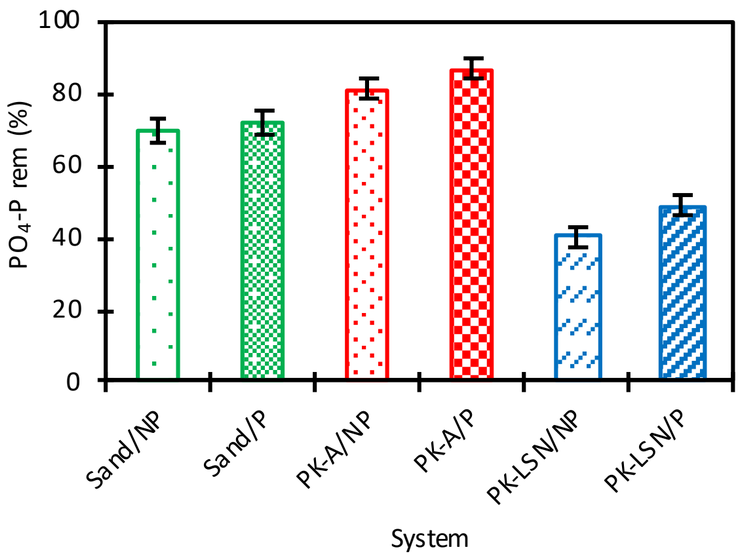

1. INTRODUCTION

Constructed Wetlands (CW) are biological engineering systems for wastewater treatment, that involve the interaction of physical, chemical and biological processes, and different removal mechanisms, which allow high removal efficiencies (Kadlec and Wallace, 2009). CWs are characterized for being robust and cost-effective technology that require low operation and maintenance efforts (Brix et al., 2007; Vymazal, 2009). CWs have been extensively investigated, demonstrating their capacity to treat diverse pollutants such as domestic, industrial, drainage mining, runoff and agriculture effluents (Reed et al., 1995; Paredes et al., 2007; Ghobrial, 2008; Nivala et al., 2012; Vymazal, 2014). CWs can be classified according to the dominant macrophytes (free-floating, floating leaved, rooted emergent and submerged), hydrology (surface or subsurface flow) and flow direction (horizontal or vertical) (Vymazal, 2010). To reduce the surface requirements, CW have evolved from passive to intensified systems, including the recent research of innovative designs that incorporate the combination with Microbial Electrochemical Technologies (MET) (Yadav et al., 2012; Doherty et al., 2015a). METs, are set-ups designed to mimic bacterial exchange of metabolic electrons with insoluble electron donors and acceptors (e.g. a solid-state electrode) through an electrical circuit (Rabaey et al., 2007). In general, METs are composed of anodic and cathodic chambers, with an aqueous solution as energy source for microorganisms, separated by a cation exchange membrane, and electrodes for stimulating the occurrence of oxidation and reduction reactions (Logan & Rabaey, 2012).

METs rely on the action of electroactive bacteria - EAB (also known as exoelectrogens, electrogens, electricegens, exoelectrogenic or anode respiring bacteria), which are microorganisms able to conserve energy from electron transfer to electrodes (Borole et al., 2011; Schröder et al., 2015). The electroactive microorganisms act as catalysts for the oxidation

of organic matter, which after consuming energy for biomass growth, release and transfer electrons, either to a conductive matrix or through an external circuit (Durruty et al., 2012). Bacteria belonging to the phylum Acidobacteria (*Geothrix*), Firmicutes (*Clostridium* and *Thermincola*) and Proteobacteria (*Rhodoferax*, *Geobacter*, *Pseudomonas* and *Shewanella*, among other genus), have been reported to develop electroactive biofilms (Logan, 2009). The most studied EAB belong to *Geobacter* and *Shewanella* genus, due to their respiratory versatility capable of using different carbon sources and electron donors/acceptors (Arends & Verstraete, 2012; Sydow et al., 2014), and their ability to oxidize organic matter from wastewater, converting its chemical energy into electric energy (Logan et al., 2006; Rozendal et al., 2008; McCarty et al., 2011). EABs have been reported in marine/fresh water sediments (Lovley, 2008; Risgaard-Petersen et al., 2014), manure (Min et al., 2005; Vilajeliu-Pons et al., 2015), aerobic/anaerobic wastewater treatment sludge (Villano et al., 2012; Gao et al., 2014), and wastewater (Escapa et al., 2014; Velvizhi & Venkata Mohan, 2015). Their presence on different environments is associated to the inherent characteristics of the electroactive microorganism, mostly anaerobic or facultative anaerobic, although there are also some species that can endure aerobic conditions (Butti et al., 2016).

MET laboratory scale experiments, like Microbial Fuel Cells (MFC) have shown potential for treating wastewater, with COD removal rates up to 90%, and coulombic efficiencies (fraction of electrons recovered as current versus the maximum possible recovery) higher than 80% (Rahimnejad et al., 2015). Despite that efficiency, several challenges exist for field applications, such as expensive electrode materials and low energy yields, constraining its implementation as a sustainable energy source (Zhang, Hu & Lee. 2016). However, from the perspective of wastewater treatment, MET systems arise as a promising alternative, capable of oxidizing easily degradable organic matter (Rabaey et al., 2007), at reported rates of around 7.1 kg COD m^{-3} d^{-1}

100 (reactor volume). Additionally, METs offer the advantage of saving aeration and/or sludge
101 disposal costs in comparison with conventional treatment systems (Wang & Ren, 2013), like
102 septic systems, activated sludge systems, among others.
103
104 The presence of redox gradients along a CW depth profile, led to explore the possibility of
105 combining CWs with MET, as done in MFC for simultaneous energy production and wastewater
106 treatment (Yadav et al., 2012). Similarly to conventional MFC, a CW-MFC is a set-up fitted with
107 an anode, located in the anaerobic zone (bottom), and a cathode in the anoxic/aerobic zone
108 (top) of a permanent flooded bed (Doherty et al., 2015a). EAB consume organic compounds in
109 the anaerobic zone and release electrons that are transferred to the anode. From the anode,
110 the electrons flow along an external circuit to the cathode, where the released electrons can be
111 used in the reduction of O_2 or NO_3. The charge balance is completed either by incorporating an
112 ion separator or by allowing the flow of ions in the bulk fluid (Ramirez-Vargas et al., 2018) (Figure
113 1). The combination of MET and CWs is a recent development, dating back to year 2012, with
114 the first experience reported with a CW-MFC laboratory scale reactor for the removal of
115 methylene blue dye, COD and simultaneous power generation from synthetic wastewater (8000
116 mg L^{-1}) at different dye concentrations (Yadav et al., 2012). The reactor operated rating in batch
117 mode, along 96 h achieving a maximal COD removal of 75% (at 1500 mg L^{-1} of initial dye
118 concentration), and maximal power and current density of 16 mW m^{-2} and 70 mA m^{-2}
119 respectively (at 1000 mg L^{-1} of initial dye concentration). Given the results reported by that first
120 study, since 2012 there has been growing an interest on testing the CW-MFC coupling.
121
122 Villaseñor et al. (2013) tested a MFC based horizontal sub-surface flow constructed wetland
123 (HSSF-CW) for treating synthetic wastewater; reached COD removal rates above 90%, with
124 power values and current density of 43 mW m^{-2} and 37 mA m^{-2}. Doherty et al. (2015b) tested

125 the removal of organic matter, nutrients and simultaneous electricity production from swine
126 slurry with alum sludge-based constructed wetlands incorporating MFC; the test included a scale
127 set-up operating with simultaneous up-flow/down-flow achieving a removal of 64% of COD, 75%
128 of NH_4, Total P (TP) up to 86%, and reaching a maximal power density of 0.27 W m^{-3}. Srivastava
129 et al., (2015) tested the performance of open and closed-circuit CW-MFC for treating synthetic
130 wastewater; in closed circuit mode reached removal efficiencies of COD from 27% to 49% higher
131 than conventional CWs, with maximal power and current densities of 321 mW m^{-3} and 422 mA
132 m^{-3}. Corbella et al. (2016) tested the removal the treatment of urban wastewater with MFCs
133 incorporated in a pilot scale CW; the removal efficiencies were 61% for COD and 60% for NH_4-
134 N, and power and current densities reached were 15 mW m^{-2} and 139 mA m^{-2}. Liu et al. (2017)
135 tested the methane mitigation and simultaneous electricity generation from synthetic
136 wastewater in a CW-MFC; this set-up operates with a HRT of 96 h was able to suppress
137 methanogenesis up to 98%, and reach a maximal power and current densities of 77 mW m^{-2} and
138 187 mA m^{-2}. Despite the number of researches focused on the CW and MFC coupling in the last
139 years (up to date are reported more than 60 research articles in Scopus® database), the majority
140 of systems have been designed at laboratory scale, and their implementation as a suitable real
141 scale wastewater treatment alternative is still in development.
142
143 Leaving aside the recovery of energy as an objective, and focusing only on the removal of
144 pollutants, an innovative development has been proposed by using electro-conductive biofilters
145 performing as a single-piece electrode, dispensing of solid-state electrodes and external circuits
146 like previously tested in CW-MFC. This new design, operating in short circuit mode resulted in
147 the development of a Microbial Electrochemical-based Constructed Wetland (METland) (Figure
148 1). In a METland system, the EAB are stimulated to generate and transfer electrons to an electro-
149 conductive material that act as an unlimited acceptor, maximizing substrate consumption,

instead of leaving free electrons for methane generation and consequently, a decrease of microbial metabolism rates (as in anaerobic system), due to the limited number of electron acceptors (Esteve-Núñez, 2015). In comparison with a CW-MFC, in a METland system the released electrons travel along the electro-conductive media instead of an external circuit (therefore operating in short circuit mode), and the ions travel with the bulk fluid to the anaerobic/anoxic zones of the system, where bacteria consortia, composed by heterotrophic and EAB communities, use them to reduce O_2 or NO_3 (Figure 1).

The METland concept has been tested for the removal of organic matter and nitrogen with HSSF coke biofilters at laboratory scale (Aguirre-Sierra et al., 2016). The coke-based biofilter showed removal rates of 91% for COD and for 96% for BOD_5 at 0.5 d HRT, and 97% for NH_4 and 69% for TN at 3.5 d HRT, results that suggest that this system can enhance biodegradation rates, thus allowing the reduction of the area requirements of classical CWs. As in CW-MFC technology, this type electroactive biofilter is still in development, therefore several uncertainties exist regarding the dynamics involve in the removal of pollutants, and its treatment performance along time. For that, this research aimed to establish the capacity to treat organic matter and nutrients in mesocosm-scale Electroactive Biofilm-Based Constructed Wetlands (EABB-CW). Apart of determining the removal efficiencies of studied pollutants, this study presents removal rate kinetics of organic matter and nutrients, which eventually could be used as reference for future studies of this type of configuration, as well as can contribute to the efforts of scaling up the technology.

2. MATERIALS AND METHODS

2.1 Experimental set-up

The experimental setup consisted of 16 columns (h: 50 cm; Ø: 16 cm; packed vol.: 8.44 L) installed at Aarhus University's greenhouses (Denmark), with temperatures ranging between 8 and 27 ºC. Twelve of the columns were filled with two types of electro-conductive materials, 6 columns for calcined petroleum coke from crushed electrodes (PK-A; Carbomax AB, Sweden), 6 columns of calcined petroleum coke with low sulphur and nitrogen content (PK-LSN; Carbomax AB, Sweden), and 4 columns filled with sand as a control (Figure 2). The physical/chemical characteristics of the materials are summarized in Table 1. Half of the columns were planted with *Juncus effusus* to determine the potential effects of the plants. The setup was up-flow fed with primary settled pig manure supplemented with starch and molasses as influent water to be treated. The feeding of the systems was done in continuous flow mode using a multi-channels peristaltic pump (LongerPump® BT100-1L). The test ran for 32 weeks, with changes of organic loading rates (OLR; Table 2) with 4 weeks of acclimation in between sampling campaigns.

2.2 Sample collection, field and laboratory analysis

After three weeks of acclimation initial period and to test the removal of organic matter and nutrients, three consecutive day sampling campaign was done, comprising the collection of grab samples from 5 different points along the height of each column (inlet and outlet). On-site measurements included pH (Hach PHC101), electrical conductivity – EC (Hach sensION+ 5060), temperature, oxygen demand – OD (Hach LDO101) and REDOX potential – Eh from water samples (Hach MTC101).

COD analysis were carried out by photometric evaluation (Hach LCI 400 cuvette test + DR 3900 spectrophotometer), BOD_5 analysis were evaluated using respirometric method (WTW

195 OxiTOP®), TSS standard methods 2540 D (APHA 2012). TN by combustion catalytic
196 oxidation/NDRI method (Shimadzu TNM-1) and PO_4 and NO_x by ion chromatography (Lachat
197 QuickChem® 8000). Additionally, to consider the impact of evapotranspiration (*ET*) on the
198 removal efficiency (*E*) of the system, water and mass balances were measured between inlet
199 and outlet according to Eq. (1) and (2).

200 $$ET = \frac{V_{in} - V_{out}}{V_{in}} \times 100\% \quad (1)$$

201

202 $$E = \frac{C_{in} \times V_{in} - C_{out} \times V_{out}}{C_{in} \times V_{in}} \times 100\% \quad (2)$$

203

204 Where V_{in} and V_{out} correspond to inlet and outlet volume (in L), C_{in} and C_{out} are the inlet and
205 outlet concentration of the assessed pollutants (in mg L^{-1}). The evapotranspiration and removal
206 efficiencies were calculated and expressed in terms of percentage.

207

208 To obtain the removal rate coefficient associated to the performance and operative condition
209 of the tested systems, the data were fitted to a first-order model (area-based) according to Eq.
210 (3).

211

212 $$\ln \frac{C_{out}}{C_{in}} = -k/HLR \quad (3)$$

213

214 Where *k* is the reaction rate coefficient and *HLR* is the Hydraulic Loading Rate (both expressed
215 as m y^{-1}). Given the upflow operation of the system, it is expected that the systems operate close
216 to a plug flow ideal reactor, therefore the first-order model was selected as the best option
217 besides has been widely used in CW as reported by Kadlec and Wallace (2009).

218

2.3 Electric potential measurements

In environments with the presence of EAB, anodic and cathodic reactions promote minor local charge imbalance creating electric fields (Risgaard-Petersen et al., 2014). In such conditions, ionic fluxes are generated, can be detected in an electrolytic conductor, and used to calculate the equivalent electron fluxes (Nielsen & Risgaard-Petersen, 2015). The ionic fluxes derived as a result of the degradation of pollutants in an EABB-CW could be quantified by measuring electric potentials (EP). The EP can be measured with sensors tailored for that purpose (Damgaard et al., 2014), and can be used as indicator of the metabolic activity of EAB. Therefore, in parallel to the estimation of the removal efficiency of organic matter, there were carried out EP test to estimate the electron fluxes inside the tested systems, to relate them with the metabolic activity of EAB and the removal of organic matter.

To measure the EP, custom-made EP sensors were used (h: 60 cm; Ø: 0.12 cm). The EP sensors are coupled to a reference electrode placed at the surface of the column, both electrodes are connected to a digital voltmeter, which through an A/D converter that transmits the signal to a PC where data is recorded (Figure 2). The ionic current density is calculated with an adapted version of Ohm's Law (Eq. 3; Nielsen & Risgaard-Petersen 2015), where *J* is the ionic/electron current density (mA cm^{-2}), σ is the electrical conductivity of water in the columns (µS cm^{-1}) and $d\Psi/dz$ the EP gradient (mV cm^{-1}).

$$J = -\sigma * d\Psi/dz \quad (4)$$

2.2 Statistical analysis

The statistical analysis was carried out using the software XLSTAT 19.02. The data were submitted to a two-way analysis of variance (two-way ANOVA) to test their statistical significance, using as explanatory variables the type of system (material + planted/non-planted)

243 and HLR. The comparison among means was tested with Tukey's HSD test with a significance
244 level of $P < 0.05$.

245 **3. RESULTS AND DISCUSSION**

246 **3.1 Removal efficiency of tested systems**

247 BOD_5 removal efficiencies of the electro-conductive materials (PK-A and PK-LSN) as well as for
248 the control systems (Sand P and NP), reached average values above 85% (Figure 3). With an OLR
249 inlet ranging from 10 to 59 g m^{-2} d^{-1}, all the tested systems (electro-conductive and control)
250 showed BOD_5 removal efficiencies between 85% and 87%. No significant differences were
251 identified between electro-conductive and control systems, neither between planted and non-
252 planted systems (Table 3 and Table 4). The good performance of the control systems could be
253 associated to the finer texture of the material used inside them. The porosity and specific surface
254 area of the sand, provide conditions for biofilm development and greater filtering effect than
255 the coarser electro-conductive materials. In contrast, the BOD removal efficiencies of the
256 electro-conductive systems are associated to the presence of EAB. The BOD removal efficiencies
257 are similar to the ones reported on previous studies dealing with electro-conductive systems,
258 such as the performance reported by Aguirre-Sierra et al. (2016), where a METland system
259 reached removal rates of 93%. Above 59 g m^{-2} d^{-1}, the performance of all tested systems declined
260 to 60% to 70% BOD_5 removal, suggesting the presence of a breaking point in the performance
261 of the electro-conductive systems around 60 g m^{-2} d^{-1}. That inlet OLR is 10-fold higher than
262 maximal recommended load in the literature for saturated systems such as horizontal-flow
263 constructed wetlands, and is comparable with the maximal suggested OLR for vertical-flow
264 constructed wetland (Dotro et al., 2017; Kadlec and Wallace, 2009).
265

Regarding COD removal, despite the bigger granulometry, the electro-conductive systems show a better performance than the control systems (Figure 3), the PK-A systems showed the highest removal performance with 90%, followed by PK-LSN systems with 85%, while the control systems reached 81%. The removal efficiencies of PK-A and PK-LSN systems are comparable to values reported by Fang et al. (2017), that with a CW-MFC was able to remove COD loads up to 90%. Similarly to BOD_5, the electro-conductive materials showed a stable performance when systems were fed with COD inlet loads ranging from 8.9 to 142 g m^{-2} d^{-1}. Whereas, at higher loads, PK-A and PK-LSN systems experienced a decrease in removal performance, falling down to 65% of COD removal. Even though there are significant differences in the performance between the tested materials (COD % removal: PK-A > PK-LSN > Sand), there are no differences between planted and non-planted systems (Table 3 and Table 4). This differs from the findings of Saz et al. (2018), where in a CW-MFC, planted systems had a better performance than non-planted systems, reaching COD removal rates between 85% to 88%. It is important to highlight that the results of organic matter removal must be taken as reference of the operation of the tested electro-conductive systems, and given that were done at mesocosm-scale, further validation at real scale is necessary.

As it may be observed, there are differences between the removal performance of BOD and COD. Meanwhile there are not significant differences for removal of BOD among systems, in terms of COD the electro-conductive systems show a better performance. It is important to remind that the BOD analysis resembles the amount of dissolved oxygen used by microorganism for oxidation of organic matter, whereas the COD measures the oxygen equivalent consumed to completely oxidize the organic matter in the water with dichromate in an acid solution. COD results can include compounds hard to oxidize biologically, inorganic compounds that can react

290 with the dichromate, or organic substances that may be toxic for microorganisms (Metcalf &
291 Eddy Inc., 2004), therefore not been able to be registered by BOD analysis.
292
293 The systems were operated under saturated regime, therefore the removal of organic matter is
294 dependent of anoxic/anaerobic processes such as denitrification, sulphate reduction or
295 methanogenesis, common pathways for organic matter removal in CW (Kadlec and Wallace,
296 2009). Under anaerobic conditions and the presence of unlimited electron acceptors like
297 electro-conductive materials, EAB belong to *Geobacter* or *Shewanella* genus would prefer to use
298 them, instead of using acceptor like Fe (III) , Mn (IV), NO_3, NO_2, S, thiosulfate, fumarate, or humic
299 substances, accelerating the consumption of organic matter (Lovley et al., 2011; Bücking et al.,
300 2013; Kracke et al., 2015). The sulfate reduction and methanogenesis processes could account
301 for a substantial fraction of COD removal in saturated CW (Dotro et al., 2017), therefore
302 explaining why the removal efficiencies of electro-conductive systems are higher than control
303 systems for COD but no for BOD.
304
305 Concerning TSS removal, the best results were obtained by the electro-conductive material PK-
306 LSN, with removal rates of 85% (non-planted) and 90% (planted). These values are higher than
307 the removal rates of Sand and PK-A system, which had a similar performance, reaching removal
308 rates between 79% and 82% (Figure 3). The higher performance of PK-LSN systems could be
309 associated to the highest porosity of the material (55%; Table 1) therefore with a higher filtration
310 capacity. Eventually, it is expected that in the long term, the electro-conductive systems
311 continue operating with similar and slightly lower performance, whereas the Sand systems is
312 expected to have a faster clogging of the media, due to the cumulative biological, physical and
313 chemical treatment process occurring inside them (Nivala et al., 2012; Liu et al., 2018; Yang et
314 al., 2018).

315 Despite of operating under saturated conditions, with limited O_2 availability the overall NH_4-N
316 removal efficiency of all the tested systems was above 39% (Figure 4). The removal efficiencies
317 were stable when the systems were fed with loading rates between 0.5 to 12.6 g m^{-2} d^{-1}, though
318 at higher loads the removal efficiency dropped to almost 0%. The highest removal rates were
319 obtained with planted systems (± 45%), without significant differences between electro-
320 conductive and the columns filled with the control materials (Table 3 and Table 4). On the other
321 hand, the removal efficiency of non-planted systems ranged between 33% and 39%, also
322 without differences between tested systems. This difference between planted and non-planted
323 systems, suggest that vegetation has an impact in terms of the removal of NH_4-N in EAAB-CW,
324 as it is reported regarding nutrient removal in conventional constructed wetlands (Brix, 1997;
325 Vymazal, 2010). NH_4-N removal efficiency is comparable with HF CWs (between 20% and 30%),
326 but lower than VF CWs (> 90%) (Dotro et al., 2017), as well as lower than other electrochemical
327 based systems, like in an Upflow CW-MFC with optional aeration at cathode, reaching NH_4-N
328 removal rates of 96% (Oon et al., 2016), or as in an air cathode CW-MFC amended with
329 dewatered alum sludge reaching removal rates between 58% and 81% (L. Xu et al., 2018).
330 Therefore, the relatively low NH_4-N removal rates of the tested systems is inherent to the
331 saturated conditions in the mesocosms, were the low O_2 available (already consumed in the
332 removal of organic matter) leads to low nitrification rates. Most of the TN removal is associated
333 to the removal of NH_4-N.
334
335 Concerning PO_4-P removal, the best performance is for PK-A/P and PK-A/NP systems with
336 removal rates ranging from 81% to 87% (Figure 4), with steady behavior regardless of the
337 different loading rates applied to the system. The removal rates of PK-A systems are significant
338 higher compared to the removal measured at the control systems (Sand/P and NP) and PK-LSN
339 systems (P and NP) (Table 3 and Table 4). It is well know that the removal of phosphorous in

340 constructed wetlands involves physical processes such as precipitation and adsorption,
341 therefore the performance of PK-A systems could be associated to their surface chemistry, by
342 the content of iron and aluminum traces (verified with Energy Dispersive X-ray spectroscopy –
343 EDS and Scanning Electron Microscopy – SEM), which could aid in the adsorption of phosphorous
344 on its surface (Kadlec and Wallace, 2009). PO_4-P removal in PK-A systems could be comparable
345 with removal efficiency of 94% reported of a CW-MFC amended with dewatered alum sludge
346 (Xu et al., 2017), or with the removal efficiency of 74% reached in an electrolysis-based
347 horizontal flow CW reported by Gao et al. (2018). The control systems (Sand/P and Sand/NP)
348 show removal efficiencies between 69% and 72%, the removal could be associated to physical
349 processes namely filtration and precipitation in the columns (Dotro et al., 2017). The lowest
350 performance is for PK-LSN systems ranging between 40% and 50%, associated to precipitation
351 processes rather than filtration or adsorption. It is also observed that for all tested materials,
352 there is better performance in planted than in non-planted systems, suggesting that plants
353 might play a role in P removal through uptake mechanism (Vymazal and Kröpfelová, 2008).
354

355 **3.2 Electron current densities from EAB metabolism and organic matter removal**

356 There is plenty of evidence of the formation of EAB biofilms and derived power or current
357 densities in MET-based set-ups. Examples of this are the findings of Beecroft et al. (2012),
358 Velvizhi et al. (2014) and Yamashita et al. (2015) that have reported the colonization of
359 electrodes by EAB in laboratory scale MFC. Similar findings have been done in MET-based CW
360 like those studied by Aguirre-Sierra et al. (2016), Li et al. (2016), J. Wang et al. (2017) and F. Xu
361 et al. (2018), which have reported the development of biofilms mainly composed by microbial
362 communities of *Proteobacteria*, *Acidobacteria* and *Firmicutes* genus, previously identified as
363 microorganisms able to build-up electro-conductive biofilms in solid-state electron acceptors
364 (Logan, 2009; Butti et al., 2016).

However, in a MET system operating as single piece electrode, i.e. without anode and cathode and external circuits, one of the main challenges to determine the presence and impact of EAB on the treatment performance, is the lack of circuits to do direct measures (e.g. with the aid of a voltmeter) of the electric current generated in the systems. Therefore, an alternative to this is was to measure electric potentials (EP) and to estimate derived ionic/electron current densities. (Figure 5).

The electric profiles measured in tested systems, provides information that indicate the development of suitable conditions for the establishment of EAB in tested electro-conductive systems, in comparison with the Sand systems. In the case of Sand systems, the average EP along the entire depth show almost constant values around 0 mV, which leads to obtain *J* densities close to 0 mA cm^{-2} (Figure 5a). This finding can be interpreted as a lack of metabolic activity associated to the presence of EAB in these systems, precisely due to the poor electroconductivity of the Sand.

On the other hand, in the systems with electro-conductive materials positive EP values were recorded, with almost constant values from the bottom of the systems (0 cm) to the middle section of them (± 20 cm), with a steady decrease from the middle section to the top of the systems (Figure 5a). This pattern leads to obtain average *J* densities of 0.091 mA cm^{-2} for PK-LSN systems, and 0.126 mA cm^{-2} for PK-A systems. In both cases, those values indicate the presence of EAB. Even though the tested electro-conductive systems were not designed to generate energy, the reported *J* densities are comparable with current densities in CW-MFC for wastewater treatment and simultaneous power generation as compiled in Ramirez-Vargas et al. (2018).

390 In previous studies dealing with the use of CW-MFC for wastewater treatment the relationship
391 between the removal of organic matter (specifically COD), and the generation of power and
392 current densities derived of the metabolic activity of EAB has been reported (Doherty et al.,
393 2015a; Ramirez-Vargas et al., 2018). Based on this, a correlation of *J* densities and the
394 performance of electro-conductive systems in terms and COD treatment, considering the
395 organic load rate at the outlet (Figure 5) was carried out. The relation between *J* density and
396 COD at effluent (g m^{-2} d^{-1}) adjust to a decreasing exponential function for both electro-
397 conductive systems, with correlation values of 0.61 for PK-LSN systems and 0.92 for PK-A
398 systems. This approach could be used to monitor the performance of electro-conductive
399 systems that uses electro-conductive materials as single piece electrode like those tested in this
400 study.

401 **3.3 Removal kinetics**

402 First-order area-based removal rate model (Eq. 3) has been applied to calculate the removal rate
403 constants (*k*) of organic matter and nutrients in an EABB-CW. Table 5 presents a summary of the
404 calculated rate constants and determination coefficients, and the relation between HLR (m y^{-1})
405 and *k* (m y^{-1}) are illustrated in Figure 6.
406
407 In terms of organic matter, the BOD_5 *k* values for PK-A systems vary between 136 m y^{-1} (planted)
408 and 143 m y^{-1} (non-planted), and for PK-LSN between 146 m y^{-1} (non-planted) and 167 m y^{-1}
409 (planted). Compared with the *k* reported by Kadlec and Wallace (2009) for a HSSF CW with a
410 primary-quality inflow (*k* = 25 m y^{-1}; 50^{th} percentile), the removal constants observed for PK-A
411 systems are between 5.4 and 5.7 times higher, and for PK-LSN system between 5.8 to 6.6 times
412 higher. If compared with a secondary-quality inflow (*k* = 37 m y^{-1}; 50^{th} percentile), the PK-A
413 systems show removal constants between 3.6 to 4 times higher, while PK-LSN systems between
414 3.9 to 4.5 times higher. The estimated removal constants could be comparable with the overall

415 *k* value reported for VF wetlands (*k* =146 m y^{-1}; 50^{th} percentile). Regarding COD, the estimated
416 removal rate constants for PK-A systems vary between 128 m y^{-1} (planted) and 139 m y^{-1} (non-
417 planted), and for PK-LSN between 104 m y^{-1} (non-planted) and 112 m y^{-1} (planted). Similarly to
418 BOD_5, the *k* values for COD are higher in comparison with previously reported values, by
419 Konnerup et al. (2009) that reported *K* values of 99 m y^{-1} and 103 m y^{-1}, for SSF CW under tropical
420 conditions planted with *Heliconia* and *Canna* respectively, or with the values reported by Trang
421 et al. (2010) with a maximal *k* value of 30 m y^{-1} for a SSF CW at a HLR equivalent to 53 m y^{-1}.
422
423 For nitrogen removal, first-order removal rate coefficients were estimated for NH_4-N and TN
424 (Table 5 and Figure 6). Regarding NH_4-N, the registered removal coefficients in PK-A systems
425 ranged from 30 m y^{-1} to 42 m y^{-1} (for non-planted and planted respectively), and for PK-LSN
426 systems between 30 m y^{-1} and 42 m y^{-1} (non-planted and planted respectively). The registered
427 areal rate coefficients are higher than the coefficient reported by Kadlec and Wallace (2009), a
428 value of 11.4 m y^{-1} (for a mean inlet NH_4-N = 40 mg L^{-1}). For both materials, the planted systems
429 presented higher removal coefficients, fact that is consequent with the registered removal
430 efficiencies of planted systems, suggesting that in electroactive systems, the plants also can play
431 a role in ammonia reduction. Likewise, the first-order area-based constants for TN are higher in
432 planted systems than in non-planted systems, supporting that planted electroactive systems can
433 have a positive effect in terms of removal of nitrogen. In the case of PK-A material, the highest
434 estimated *k* values are 24 m y^{-1} for planted system and 14 m y^{-1} for non-planted system. For PK-
435 LSN material, the *k* values estimated are 29 m y^{-1} and 23 m y^{-1} for planted and non-planted
436 systems. The removal rate coefficients of TN for PK-A and PK-LSN systems are higher than the
437 values reported by Kadlec and Wallace (2009) (*k* = 8.4 m y^{-1}; mean TN inlet = 83.8 mg L^{-1}; 50^{th}
438 percentile) or by Konnerup et al. (2009) (*k* = 5.77 m y^{-1} ; mean TN inlet = 22,9 mg L^{-1}), but similar
439 to the maximal value reported by Trang et al. (2010) (*k* = 24 m y^{-1} ; HLR = 6.2 cm d^{-1}).

440 In terms of phosphorous, the calculated removal rate coefficients for PO_4-P show higher values
441 in tested systems containing PK-A material, than in systems with PK-LSN material. In the case of
442 PK-A systems, the *k* values varied between 131 m y^{-1} (non-planted) and 146 m y^{-1} (planted);
443 whereas for PK-LSN systems, the obtained *k* values ranged between 48 m y^{-1} (non-planted) and
444 64 m y^{-1} (planted). For both materials, the planted systems showed higher removal rate
445 constants in comparison with non-planted systems, suggesting that the removal efficiency is
446 associated to plant uptake mechanism. The estimated PO_4-P reaction coefficients of PK-A and
447 PK-LSN are higher than those reported for TP by Konnerup et al. (2009) (*k* = 5.43 m y^{-1}; mean TP
448 = 8. 55 mg L^{-1}; mean PO_4-P = 6 mg L^{-1}) and Trang et al. (2010) (*k* = 84 m y^{-1}; HLR = 6.2 cm d^{-1}).

449 **4. CONCLUSIONS**

450 The EABB-CW tested in this study was successful and showed to be a promising for treating
451 wastewaters combining constructed wetlands and microbial electrochemical technologies, but
452 instead of operating with electrodes and external circuits like in a classical MFC, it uses the
453 support media (electro-conductive materials) as a single-piece electrode.

454

455 With the EABB-CW systems tested in this study, reached overall removal efficiencies of 88% for
456 BOD_5, 90% for COD, 46% for NH_4-N, and 86% for PO_4-P. In terms of BOD_5 there are not
457 differences between tested systems, whereas for COD, the PK-A systems showed the best
458 performance, followed by PK-LSN systems; no significant differences were detected between
459 planted and non-planted systems. In regards of organic matter removal as BOD_5 and COD, the
460 registered efficiencies were achieved even at loading rates 5 and 10-fold higher than
461 recommended values for VF and HFCWs respectively.

462

463 Regarding NH_4-N, the removal efficiencies are comparable with HFCWs but lower in comparison
464 with VFCWs, given the low O_2 available when EABB-CW is operated under saturated conditions.
465 The significant differences between planted and non-planted systems, suggests that plants also
466 play a role in NH_4-N removal in EABB-CW like in conventional CWs.
467
468 The PO_4-P removal is significant higher in EABB-CW using PK-A material in comparison with PK-
469 LSN and control systems. The higher removal efficiency could be more associated to the
470 chemical characteristics of the material, presumably by the presence of iron traces at its surface,
471 promoting the removal by adsorption. Also, the plants seem to play a role in the PO_4-P, given
472 that planted systems showed a higher performance than non-planted systems.
473
474 The removal performance of tested EABB-CWs can be corroborated by the calculated values of
475 the first-order area-based removal rate constants. The *k* values for organic matter and nutrients
476 are higher in tested EABB-CWs, than the values commonly reported in literature for HF and VF
477 CWs, fact that open the possibility of exploring the potential of using EABB-CW at higher inlet
478 loading rates, leading to the reduction of necessary surface are for its implementation.
479
480 The measured ionic current densities (*J*) are higher in electro-conductive systems than in control
481 systems (no current registered). These differences could be associated with the development of
482 electroactive biofilms, which might be related with the relatively higher removal rates of organic
483 matter in PK-A and PK-LSN systems in comparison with control systems. Therefore, *J* values
484 could be used as indicator of the performance of EABB-CWs.
485
486 Ongoing and future will invest efforts in e monitoring a real scale system based on EABB-CW
487 concept already in operation, as well as in exploring the development of operational

488 modifications to improve nitrification and denitrification that will redound in better total
489 nitrogen removal.

490 **ACKNOWLEDGEMENTS**

491

492 This study has been supported with resources of the project “iMETland: A new generation of
493 Microbial Electrochemical Wetland for effective decentralized wastewater treatment systems”,
494 funded by European Union’s Horizon 2020 research and innovation programme (grant
495 agreement No. 642190). Carlos A. Ramirez-Vargas kindly acknowledges to the Administrative
496 Department of Science and Technology of Colombia (COLCIENCIAS) for granting his PhD
497 scholarship (conv. 646/2014). Special thanks to Lone J. Ottosen, Malin Camilla Håckansson and
498 Ole Zahrtmann for their support in laboratory analysis and experimental set-up. Also to Amanda
499 Prado from IMDEA Water (Spain) for her support in the analysis of the electroconductive
500 materials with Energy Dispersive X-ray spectroscopy (EDS) and Scanning Electrode Microscopy
501 (SEM).

502 **REFERENCES**

503

504 Aguirre-Sierra, A., Bacchetti De Gregoris, T., Berná, A., Salas, J.J., Aragón, C., Esteve-Núñez, A.,
505 2016. Microbial Electrochemical Systems outperform fixed-bed biofilters for cleaning-up
506 urban wastewater. Environ. Sci. Water Res. Technol. 2, 4435–4448.
507 doi:10.1039/c1ee01745d
508 Arends, J.B.A., Verstraete, W., 2012. 100 Years of Microbial Electricity Production: Three
509 Concepts for the Future. Microb. Biotechnol. 5, 333–346. doi:10.1111/j.1751-
510 7915.2011.00302.x

511 Beecroft, N.J., Zhao, F., Varcoe, J.R., Slade, R.C.T., Thumser, A.E., Avignone-Rossa, C., 2012.
512 Dynamic changes in the microbial community composition in microbial fuel cells fed with
513 sucrose. Appl. Microbiol. Biotechnol. 93, 423–437. doi:10.1007/s00253-011-3590-y
514 Borole, A.P., Reguera, G., Ringeisen, B., Wang, Z.-W., Feng, Y., Kim, B.H., 2011. Electroactive
515 biofilms: Current status and future research needs. Energy Environ. Sci. 4, 4813.
516 doi:10.1039/c1ee02511b
517 Brix, H., 1997. Do macrophytes play a role in constructed treatment wetlands? Water Sci.
518 Technol. doi:10.1016/S0273-1223(97)00047-4
519 Bücking, C., Schicklberger, M., Gescher, J., 2013. The Biochemistry of Dissimilatory Ferric Iron
520 and Manganese Reduction in Shewanella oneidensis, in: Microbial Metal Respiration: From
521 Geochemistry to Potential Applications. pp. 49–82. doi:10.1007/978-3-642-32867-1
522 Butti, S.K., Velvizhi, G., Sulonen, M.L.K., Haavisto, J.M., Oguz Koroglu, E., Yusuf Cetinkaya, A.,
523 Singh, S., Arya, D., Annie Modestra, J., Vamsi Krishna, K., Verma, A., Ozkaya, B., Lakaniemi,
524 A.-M., Puhakka, J.A., Venkata Mohan, S., 2016. Microbial electrochemical technologies
525 with the perspective of harnessing bioenergy: Maneuvering towards upscaling. Renew.
526 Sustain. Energy Rev. 53, 462–476. doi:10.1016/j.rser.2015.08.058
527 Corbella, C., Garfí, M., Puigagut, J., 2016. Long-term assessment of best cathode position to
528 maximise microbial fuel cell performance in horizontal subsurface flow constructed
529 wetlands. Sci. Total Environ. 563–564, 448–455. doi:10.1016/j.scitotenv.2016.03.170
530 Damgaard, L.R., Risgaard-Petersen, N., Nielsen, L.P., 2014. Electric potential microelectrode for
531 studies of electrobiogeophysics. J. Geophys. Res. G Biogeosciences 119, 1906–1917.
532 doi:10.1002/2014JG002665
533 Doherty, L., Zhao, Y., Zhao, X., Hu, Y., Hao, X., Xu, L., Liu, R., 2015a. A review of a recently
534 emerged technology: Constructed wetland – microbial fuel cells. Water Res.
535 doi:10.1016/j.watres.2015.08.016

536 Doherty, L., Zhao, Y., Zhao, X., Wang, W., 2015b. Nutrient and organics removal from swine
537 slurry with simultaneous electricity generation in an alum sludge-based constructed
538 wetland incorporating microbial fuel cell technology. Chem. Eng. J. 266, 74–81.
539 doi:10.1016/j.cej.2014.12.063
540 Dotro, G., Molle, P., Nivala, J., Puigagut, J., Stein, O., 2017. Treatment Wetlands, First. ed. IWA
541 Publishing, London.
542 Durruty, I., Bonanni, P.S., González, J.F., Busalmen, J.P., 2012. Evaluation of potato-processing
543 wastewater treatment in a microbial fuel cell. Bioresour. Technol. 105, 81–7.
544 doi:10.1016/j.biortech.2011.11.095
545 Escapa, A., San-Martín, M.I., Morán, A., 2014. Potential Use of Microbial Electrolysis Cells in
546 Domestic Wastewater Treatment Plants for Energy Recovery. Front. Energy Res. 2, 1–10.
547 doi:10.3389/fenrg.2014.00019
548 Esteve-Núñez, A., 2015. Electricity-generating bacteria Bioelectrogenesis : sustainable
549 biotechnology. Int. Innov. 181, 109–111.
550 Fang, Z., Cheng, S., Cao, X., Wang, H., Li, X., 2017. Effects of electrode gap and wastewater
551 condition on the performance of microbial fuel cell coupled constructed wetland. Environ.
552 Technol. (United Kingdom) 38, 1051–1060. doi:10.1080/09593330.2016.1217280
553 Gao, C., Wang, A., Wu, W.-M., Yin, Y., Zhao, Y.-G., 2014. Enrichment of anodic biofilm inoculated
554 with anaerobic or aerobic sludge in single chambered air-cathode microbial fuel cells.
555 Bioresour. Technol. 167, 124–32. doi:10.1016/j.biortech.2014.05.120
556 Gao, Y., Zhang, W., Gao, B., Jia, W., Miao, A., Xiao, L., Yang, L., 2018. Highly efficient removal of
557 nitrogen and phosphorus in an electrolysis-integrated horizontal subsurface-flow
558 constructed wetland amended with biochar. Water Res. 139, 301–310.
559 doi:10.1016/J.WATRES.2018.04.007
560 Kadlec, R., Wallace, S., 2009. Treatment wetlands, Second. ed. CRC Press, Boca Raton, FL.

561 Konnerup, D., Koottatep, T., Brix, H., 2009. Treatment of domestic wastewater in tropical,
562 subsurface flow constructed wetlands planted with Canna and Heliconia. Ecol. Eng. 35,
563 248–257. doi:10.1016/J.ECOLENG.2008.04.018
564 Kracke, F., Vassilev, I., Krömer, J.O., 2015. Microbial electron transport and energy conservation
565 - the foundation for optimizing bioelectrochemical systems. Front. Microbiol. 6, 1–18.
566 doi:10.3389/fmicb.2015.00575
567 Liu, H., Hu, Z., Zhang, J., Ji, M., Zhuang, L., Nie, L., Liu, Z., 2018. Effects of solids accumulation and
568 plant root on water flow characteristics in horizontal subsurface flow constructed wetland.
569 Ecol. Eng. 120, 481–486. doi:10.1016/J.ECOLENG.2018.07.003
570 Liu, S., Feng, X., Li, X., 2017. Bioelectrochemical approach for control of methane emission from
571 wetlands. Bioresour. Technol. 241, 812–820. doi:10.1016/j.biortech.2017.06.031
572 Logan, B.E., 2009. Exoelectrogenic bacteria that power microbial fuel cells. Nat. Rev. Microbiol.
573 7, 375–381. doi:10.1038/nrmicro2113
574 Logan, B.E., Hamelers, B., Rozendal, R., Schröder, U., Keller, J., Freguia, S., Aelterman, P.,
575 Verstraete, W., Rabaey, K., 2006. Microbial fuel cells: Methodology and technology.
576 Environ. Sci. Technol. 40, 5181–5192. doi:10.1021/es0605016
577 Logan, B.E., Rabaey, K., 2012. Conversion of Wastes into Bioelectricity and Chemicals by Using
578 Microbial Electrochemical Technologies. Science (80-.). 337, 686–689.
579 doi:10.1126/science.1217412
580 Lovley, D.R., 2008. Extracellular electron transfer: Wires, capacitors, iron lungs, and more.
581 Geobiology 6, 225–231. doi:10.1111/j.1472-4669.2008.00148.x
582 Lovley, D.R., Ueki, T., Zhang, T., Malvankar, N.S., Shrestha, P.M., Flanagan, K.A., Aklujkar, M.,
583 Butler, J.E., Giloteaux, L., Rotaru, A.-E., Holmes, D.E., Franks, A.E., Orellana, R., Risso, C.,
584 Nevin, K.P., 2011. Geobacter: The Microbe Electric's Physiology, Ecology, and Practical
585 Applications, 1st ed, Advances in Microbial Physiology. Elsevier Ltd. doi:10.1016/B978-0-

12-387661-4.00004-5

McCarty, P.L., Bae, J., Kim, J., 2011. Domestic wastewater treatment as a net energy producer-can this be achieved? Environ. Sci. Technol. 45, 7100–7106. doi:10.1021/es2014264

Metcalf & Eddy Inc., 2004. Wastewater Engineering: Treatment and Reuse, Fourt. ed. McGraw-Hill, New York.

Min, B., Kim, J., Oh, S., Regan, J.M., Logan, B.E., 2005. Electricity generation from swine wastewater using microbial fuel cells. Water Res. 39, 4961–8. doi:10.1016/j.watres.2005.09.039

Nielsen, L.P., Risgaard-Petersen, N., 2015. Rethinking Sediment Biogeochemistry After the Discovery of Electric Currents. Ann. Rev. Mar. Sci. 7, 425–442. doi:10.1146/annurev-marine-010814-015708

Nivala, J., Knowles, P., Dotro, G., García, J., Wallace, S., 2012. Clogging in subsurface-flow treatment wetlands: Measurement, modeling and management. Water Res. 46, 1625–1640. doi:10.1016/J.WATRES.2011.12.051

Oon, Y.-L., Ong, S.-A., Ho, L.-N., Wong, Y.-S., Dahalan, F.A., Oon, Y.-S., Lehl, H.K., Thung, W.-E., 2016. Synergistic effect of up-flow constructed wetland and microbial fuel cell for simultaneous wastewater treatment and energy recovery. Bioresour. Technol. 203, 190–197. doi:10.1016/j.biortech.2015.12.011

Rabaey, K., Rodríguez, J., Blackall, L.L., Keller, J., Gross, P., Batstone, D., Verstraete, W., Nealson, K.H., 2007. Microbial ecology meets electrochemistry: electricity-driven and driving communities. ISME J. 1, 9–18. doi:10.1038/ismej.2007.4

Rabaey, K., Rozendal, R.A., 2010. Microbial electrosynthesis — revisiting the electrical route for microbial production 8. doi:10.1038/nrmicro2422

Rahimnejad, M., Adhami, A., Darvari, S., Zirepour, A., Oh, S.-E., 2015. Microbial fuel cell as new technology for bioelectricity generation: A review. Alexandria Eng. J. 54, 745–756.

611 doi:10.1016/j.aej.2015.03.031
612 Ramirez-Vargas, C.A., Prado, A., Arias, C.A., Carvalho, P.N., Esteve-Núñez, A., Brix, H., 2018.
613 Microbial electrochemical technologies for wastewater treatment : principles and
614 evolution from microbial fuel cells to bioelectrochemical-based constructed wetlands.
615 Water 10, 1–29. doi:https://doi.org/10.3390/w10091128
616 Risgaard-Petersen, N., Damgaard, L.R., Revil, A., Nielsen, L.P., 2014. Mapping electron sources
617 and sinks in a marine biogeobattery. J. Geophys. Res. G Biogeosciences 119, 1475–1486.
618 doi:10.1002/2014JG002673
619 Rozendal, R.A., Hamelers, H.V.M., Rabaey, K., Keller, J., Buisman, C.J.N., 2008. Towards practical
620 implementation of bioelectrochemical wastewater treatment. Trends Biotechnol. 26, 450–
621 459. doi:10.1016/j.tibtech.2008.04.008
622 Saz, Ç., Türe, C., Türker, O.C., Yakar, A., 2018. Effect of vegetation type on treatment
623 performance and bioelectric production of constructed wetland modules combined with
624 microbial fuel cell (CW-MFC) treating synthetic wastewater. Environ. Sci. Pollut. Res. 25,
625 8777–8792.
626 Schröder, U., Harnisch, F., Angenent, L.T., 2015. Microbial electrochemistry and technology:
627 terminology and classification. Energy Environ. Sci. 8, 513–519. doi:10.1039/C4EE03359K
628 Srivastava, P., Yadav, A.K., Mishra, B.K., 2015. The effects of microbial fuel cell integration into
629 constructed wetland on the performance of constructed wetland. Bioresour. Technol. 195,
630 223–30. doi:10.1016/j.biortech.2015.05.072
631 Sydow, A., Krieg, T., Mayer, F., Schrader, J., Holtmann, D., 2014. Electroactive bacteria -
632 molecular mechanisms and genetic tools. Appl. Microbiol. Biotechnol. 98, 8481–8495.
633 doi:10.1007/s00253-014-6005-z
634 Trang, N.T.D., Konnerup, D., Schierup, H.H., Chiem, N.H., Tuan, L.A., Brix, H., 2010. Kinetics of
635 pollutant removal from domestic wastewater in a tropical horizontal subsurface flow

636 constructed wetland system: Effects of hydraulic loading rate. Ecol. Eng. 36, 527–535.
637 doi:10.1016/j.ecoleng.2009.11.022
638 Velvizhi, G., Goud, R.K., Venkata Mohan, S., 2014. Anoxic bio-electrochemical system for
639 treatment of complex chemical wastewater with simultaneous bioelectricity generation.
640 Bioresour. Technol. 151, 214–220. doi:10.1016/j.biortech.2013.10.028
641 Velvizhi, G., Venkata Mohan, S., 2015. Bioelectrogenic role of anoxic microbial anode in the
642 treatment of chemical wastewater: Microbial dynamics with bioelectro-characterization.
643 Water Res. 70, 52–63. doi:10.1016/j.watres.2014.11.002
644 Vilajeliu-Pons, A., Puig, S., Pous, N., Salcedo-Dávila, I., Bañeras, L., Balaguer, M.D., Colprim, J.,
645 2015. Microbiome characterization of MFCs used for the treatment of swine manure. J.
646 Hazard. Mater. 288, 60–8. doi:10.1016/j.jhazmat.2015.02.014
647 Villano, M., Aulenta, F., Beccari, M., Majone, M., 2012. Start-up and performance of an activated
648 sludge bioanode in microbial electrolysis cells. Chem. Eng. Trans. 27, 109–114.
649 doi:10.3303/CET1227019
650 Villaseñor, J., Capilla, P., Rodrigo, M.A., Cañizares, P., Fernández, F.J., 2013. Operation of a
651 horizontal subsurface flow constructed wetland--microbial fuel cell treating wastewater
652 under different organic loading rates. Water Res. 47, 6731–8.
653 doi:10.1016/j.watres.2013.09.005
654 Vymazal, J., 2010. Constructed Wetlands for Wastewater Treatment. Water 2, 530–549.
655 doi:10.3390/w2030530
656 Vymazal, J., Kröpfelová, L., 2008. Wastewater Treatment in Constructed Wetlands with
657 Horizontal Sub-Surface Flow. Environmental Pollution, vol 14, First. ed. Springer,
658 Dordrecht.
659 Wang, H., Ren, Z.J., 2013. A comprehensive review of microbial electrochemical systems as a
660 platform technology. Biotechnol. Adv. 31, 1796–807.

661 doi:10.1016/j.biotechadv.2013.10.001
662 Wang, J., Song, X., Wang, Y., Abayneh, B., Li, Y., Yan, D., Bai, J., 2016. Nitrate removal and
663 bioenergy production in constructed wetland coupled with microbial fuel cell:
664 Establishment of electrochemically active bacteria community on anode. Bioresour.
665 Technol. 221, 358–365. doi:10.1016/j.biortech.2016.09.054
666 Wang, J., Song, X., Wang, Y., Bai, J., Li, M., Dong, G., Lin, F., Lv, Y., Yan, D., 2017. Bioenergy
667 generation and rhizodegradation as affected by microbial community distribution in a
668 coupled constructed wetland-microbial fuel cell system associated with three
669 macrophytes. Sci. Total Environ. 607–608, 53–62. doi:10.1016/J.SCITOTENV.2017.06.243
670 Xu, F., Cao, F., Kong, Q., Zhou, L., Yuan, Q., Zhu, Y., Wang, Q., Du, Y., Wang, Z., 2018. Electricity
671 production and evolution of microbial community in the constructed wetland-microbial
672 fuel cell. Chem. Eng. J. 339, 479–486. doi:10.1016/J.CEJ.2018.02.003
673 Xu, L., Zhao, Y., Wang, T., Liu, R., Gao, F., 2017. Energy capture and nutrients removal
674 enhancement through a stacked constructed wetland incorporated with microbial fuel cell.
675 Water Sci. Technol. 76. doi:10.2166/wst.2017.168
676 Xu, L., Zhao, Y., Wang, X., Yu, W., 2018. Applying multiple bio-cathodes in constructed wetland-
677 microbial fuel cell for promoting energy production and bioelectrical derived nitrification-
678 denitrification process. Chem. Eng. J. 344, 105–113. doi:10.1016/J.CEJ.2018.03.065
679 Yadav, A.K., Dash, P., Mohanty, A., Abbassi, R., Mishra, B.K., 2012. Performance assessment of
680 innovative constructed wetland-microbial fuel cell for electricity production and dye
681 removal. Ecol. Eng. 47, 126–131. doi:10.1016/j.ecoleng.2012.06.029
682 Yakar, A., Türe, C., Türker, O.C., Vymazal, J., Saz, Ç., 2018. Impacts of various filtration media on
683 wastewater treatment and bioelectric production in up-flow constructed wetland
684 combined with microbial fuel cell (UCW-MFC). Ecol. Eng. 117, 120–132.
685 doi:10.1016/J.ECOLENG.2018.03.016

686 Yamashita, T., Ishida, M., Ogino, A., Yokoyama, H., 2015. Evaluation of organic matter removal
687 and electricity generation by using integrated microbial fuel cells for wastewater
688 treatment. Environ. Technol. 3330, 1–20. doi:10.1080/09593330.2015.1066874
689 Yang, M., Lu, M., Bian, H., Sheng, L., He, C., 2018. Effects of physical clogging on the performance
690 of a lab-scale vertical subsurface flow constructed wetland system and simulation
691 research. Ecol. Indic. 92, 11–17. doi:10.1016/J.ECOLIND.2017.05.058
692 Zhang, Q., Hu, J., Lee, D.-J., 2016. Microbial fuel cells as pollutant treatment units: Research
693 updates. Bioresour. Technol. doi:10.1016/j.biortech.2016.02.00

STOTEN-D18-05566 - Captions for figures

Figure 1. Typical constructed wetland–microbial fuel cell (CW-MFC) configuration (left); Conceptual illustration of METland setup (right) (Ramirez-Vargas et al., 2018).

Figure 1. EABB-CW column set-up. (a) Set-up for wastewater treatment analysis. (b) Set-up complemented with sensors and meters for electric potential measures; (c) Electro-conductive materials (PK-A and PK-LSN), Sand (control) and plants used in this study.

Figure 3. Global mass removal efficiency (%) of organic matter (BOD_5, and COD) and TSS. PK-A: electro-conductive material PK-A; PK-LSN: electro-conductive material PK-LSN; Sand: control material; P: planted; NP: non-planted.

Figure 4. Global mass removal efficiency (%) of NH_4-N, TN and PO_4-P by tested system. PK-A: electro-conductive material PK-A; PK-LSN: electro-conductive material PK-LSN; Sand: control material; P: planted; NP: non-planted.

Figure 5 Indicator of presence of EAB in tested systems. (a) Average EP profiles of PK-A, PK-LSN and Sand systems and derived ionic current density - J (mA cm^{-2}); non-linear correlation between ionic current density - J (mA cm^{-2}) and outlet COD load for PK-A systems (b) and PK-LSN systems (c). Each dot represents an EP test.

Figure 6. Fitted curves of first-order area-based removal rate constant (k) vs. inlet HLR of BOD_5, COD, NH_4-N and PO_4-P. Each point represents the mean value of 18 observations per HLR and tested system.

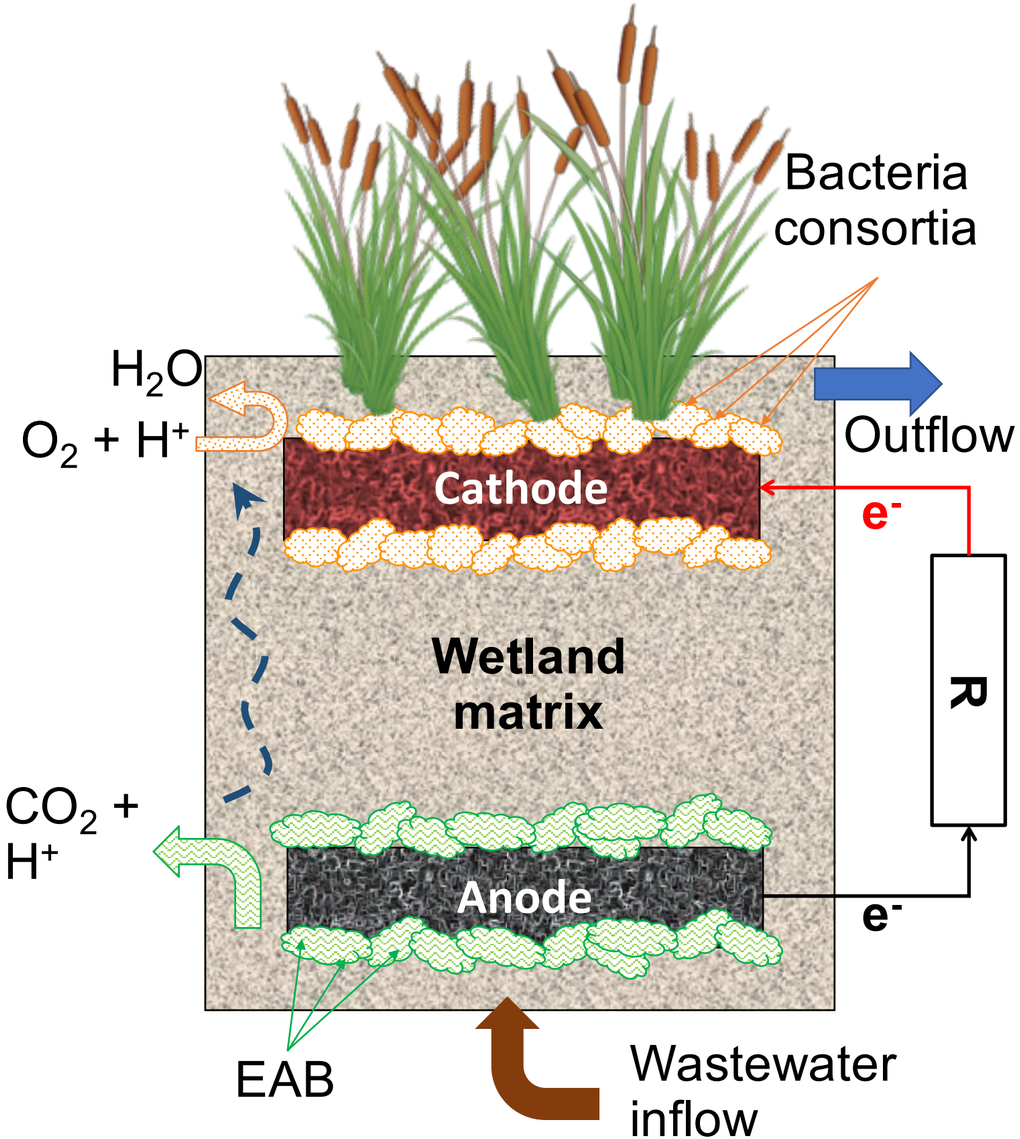
Bacteria consortia
H_2O
$O_2 + H^+$
Outflow
Cathode
e^-
R
Wetland matrix
$CO_2 + H^+$
Anode
e^-
EAB
Wastewater inflow

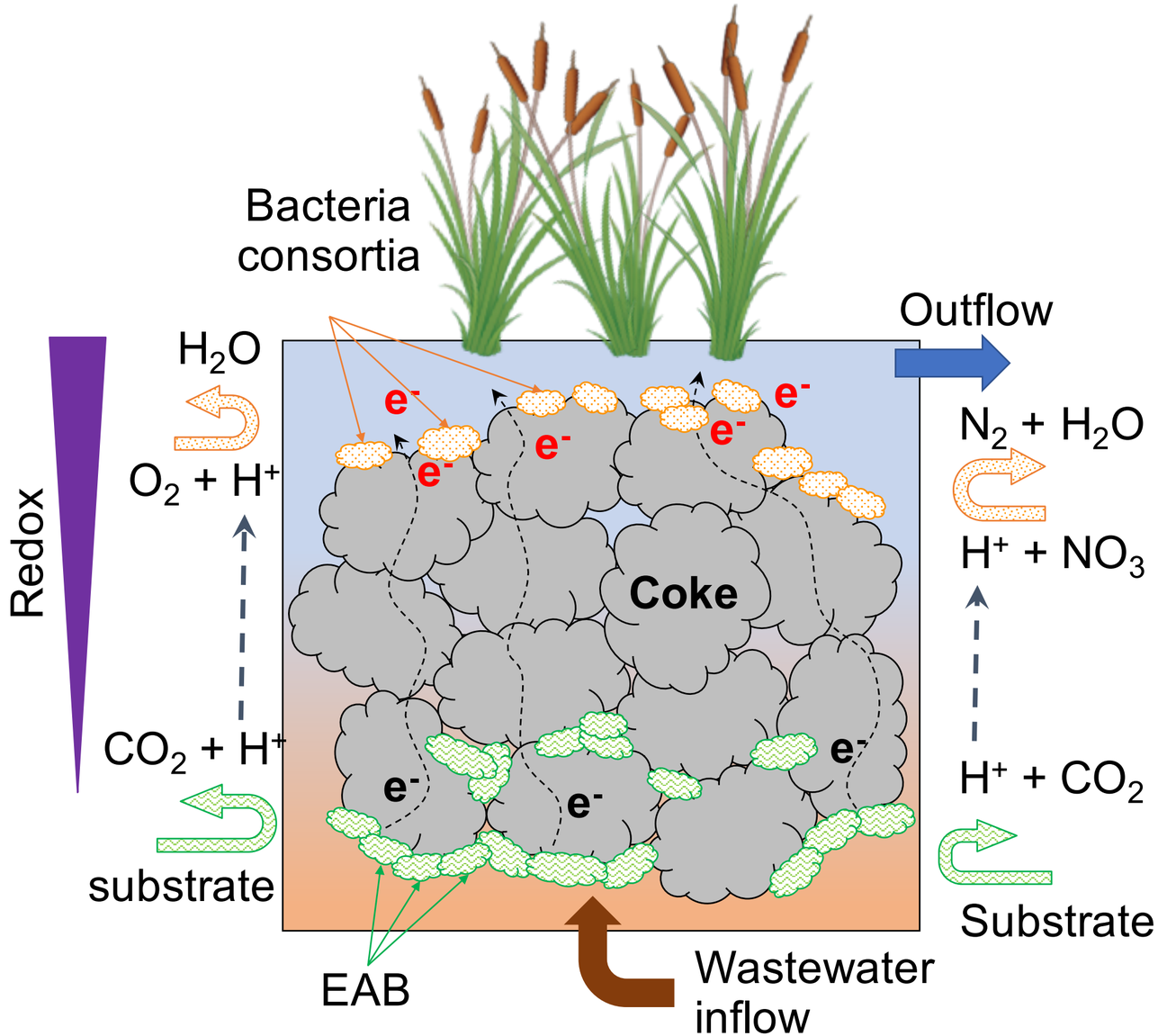
Bacteria consortia
Outflow
Redox
H_2O
$O_2 + H^+$
e^-
$N_2 + H_2O$
$H^+ + NO_3$
Coke
$CO_2 + H^+$
substrate
$H^+ + CO_2$
Substrate
EAB
Wastewater inflow

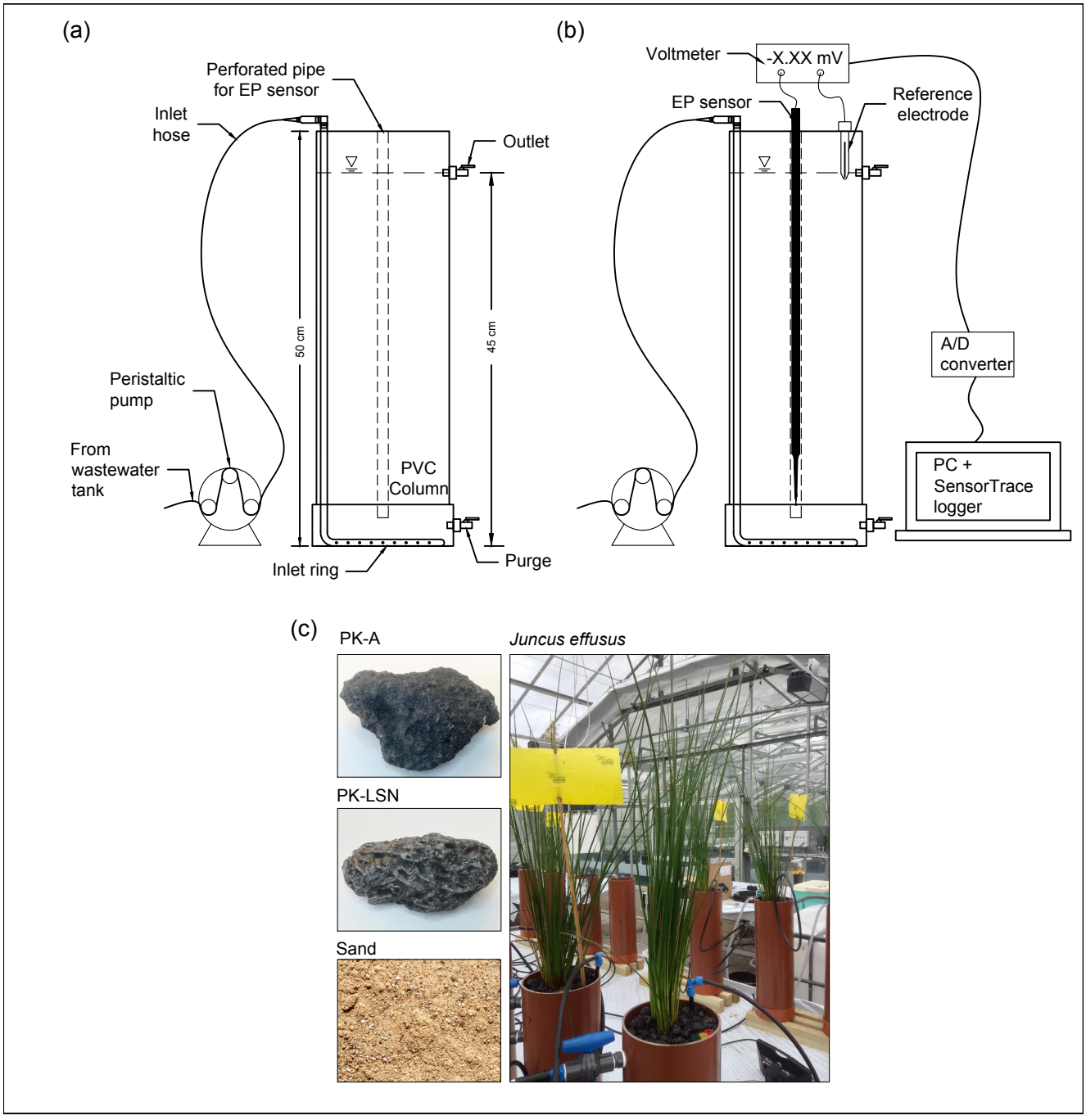
(a)
Perforated pipe for EP sensor
Inlet hose
Outlet
50 cm
45 cm
Peristaltic pump
From wastewater tank
PVC Column
Inlet ring
Purge
(b)
Voltmeter
-X.XX mV
EP sensor
Reference electrode
A/D converter
PC + SensorTrace logger
(c)
PK-A
PK-LSN
Sand
Juncus effusus

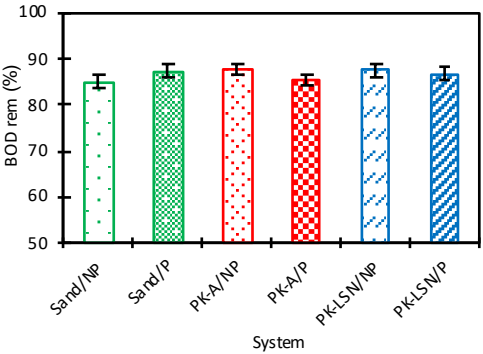
100
90
80
70
60
50
BOD rem (%)
Sand/NP
Sand/P
PK-A/NP
PK-A/P
PK-LSN/NP
PK-LSN/P
System

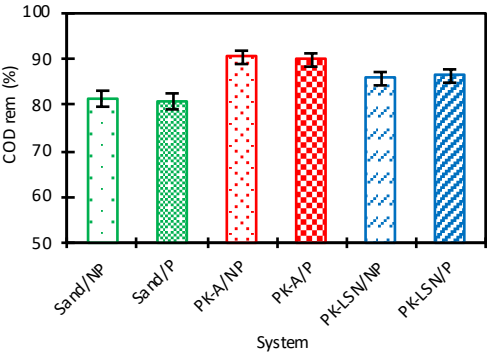
100
90
80
70
60
50
COD rem (%)
Sand/NP
Sand/P
PK-A/NP
PK-A/P
PK-LSN/NP
PK-LSN/P
System

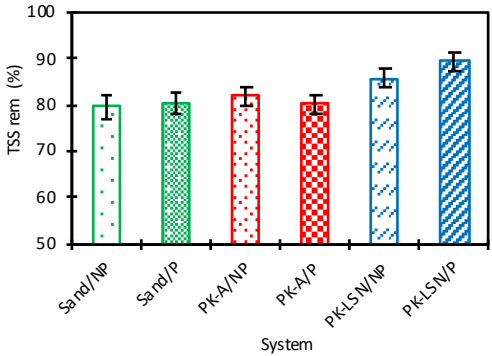
100
90
80
70
60
50
TSS rem (%)
Sand/NP
Sand/P
PK-A/NP
PK-A/P
PK-LSN/NP
PK-LSN/P
System

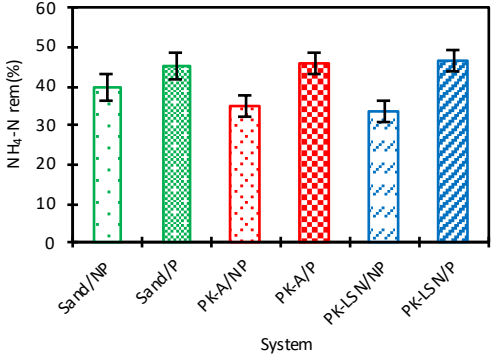
60
50
40
30
20
10
0
NH4-N rem (%)
Sand/NP
Sand/P
PK-A/NP
PK-A/P
PK-LSN/NP
PK-LSN/P
System

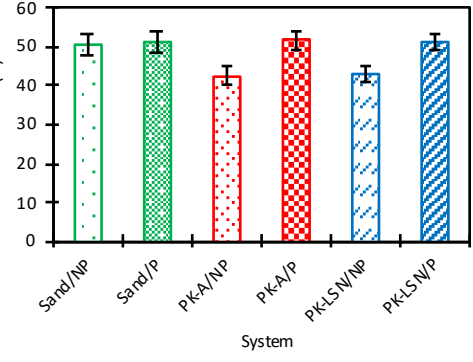
60
50
40
30
20
10
0
TN rem (%)
Sand/NP
Sand/P
PK-A/NP
PK-A/P
PK-LSN/NP
PK-LSN/P
System

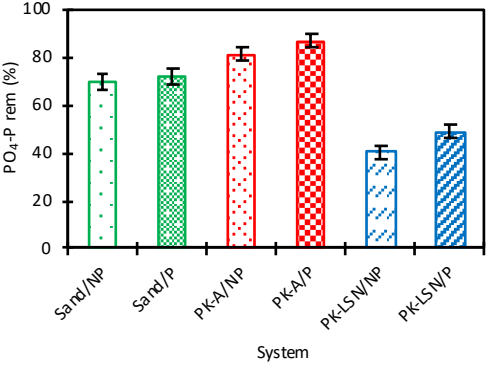
100
80
60
40
20
0
PO4-P rem (%)
Sand/NP
Sand/P
PK-A/NP
PK-A/P
PK-LSN/NP
PK-LSN/P
System

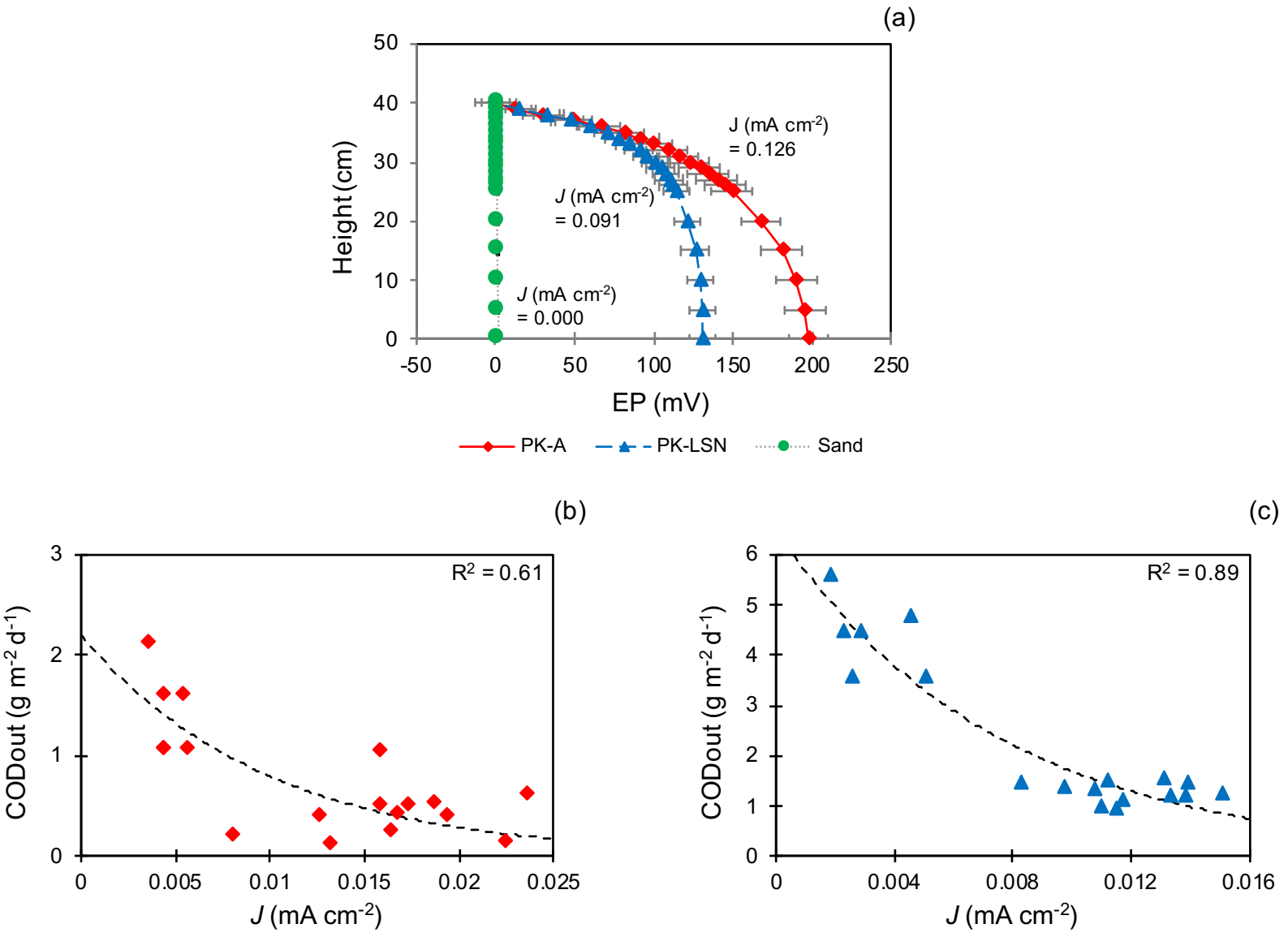
(a)
Height (cm)
EP (mV)
J (mA cm-2) = 0.126
J (mA cm-2) = 0.091
J (mA cm-2) = 0.000
PK-A
PK-LSN
Sand
(b)
R2 = 0.61
CODout (g m-2 d-1)
J (mA cm-2)
(c)
R2 = 0.89
CODout (g m-2 d-1)
J (mA cm-2)

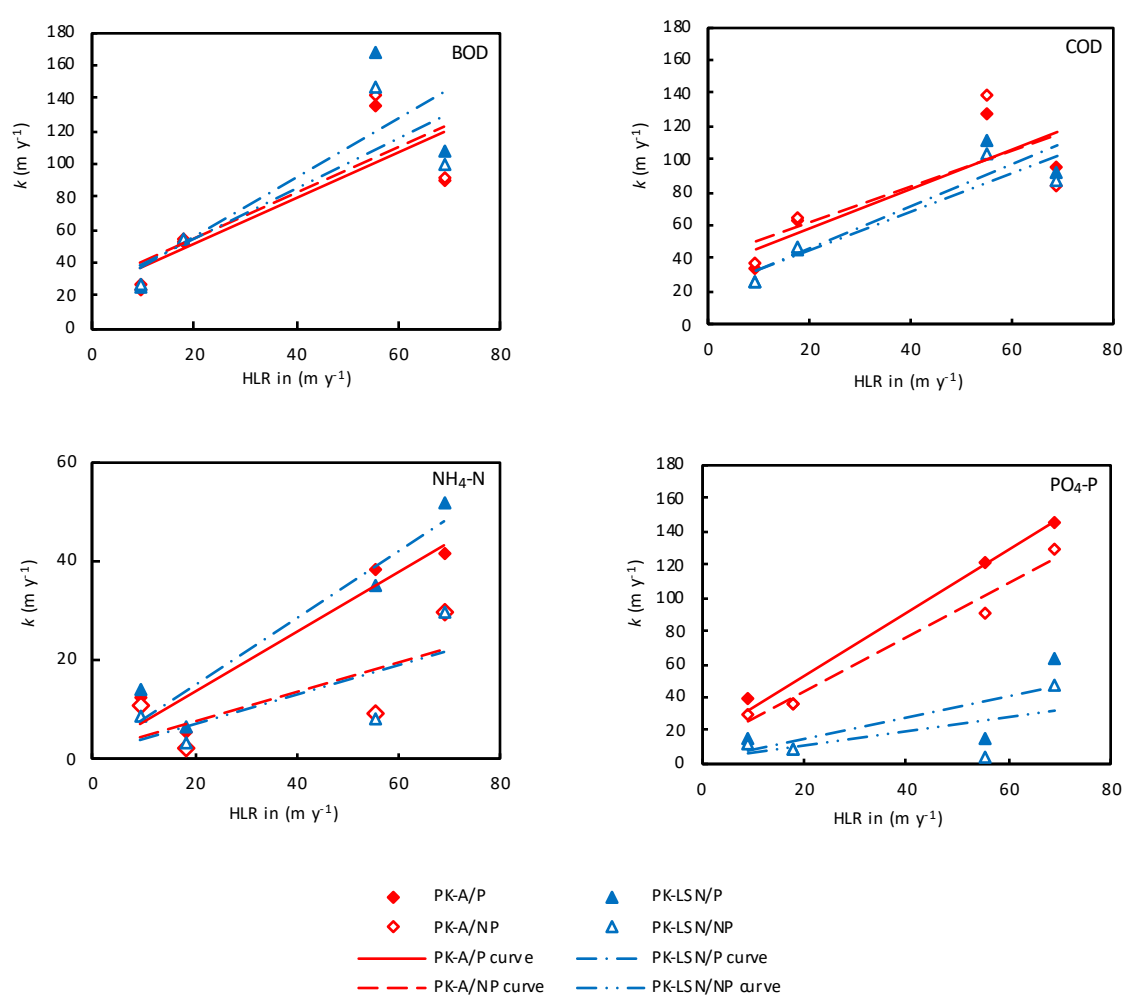
BOD
COD
NH4-N
PO4-P
k (m y-1)
HLR in (m y-1)
PK-A/P
PK-A/NP
PK-LSN/P
PK-LSN/NP
PK-A/P curve
PK-A/NP curve
PK-LSN/P curve
PK-LSN/NP curve

Table 1. Physical-chemical characteristic of filter materials used in this study.

Parameter	Units	PK-A*	PK-LSN*	Sand**
Carbon-fix[†]	%	95.80	99.43	-
Sulfur[†]	%	1.80	0.54	-
Nitrogen[†]	%	1.00	0.375	-
Ash[†]	%	2.00	0.07	-
Volatiles[†]	%	0.50	0.50	-
H_2O[†]	%	0.20	0.50	-
Resistivity	Ω-m	0.0227	0.0262	-
Porosity	%	39 ± 1.63	55 ± 2.55	38 ± 2.00
Density	g ml^{-1}	1.95 ± 0.09	1.61 ± 0.06	2.62 ± 0.01
D_{10}	mm	9.47	3.23	0.46
D_{60}	mm	22.93	20.15	1.18
Iron[††]	-	Detected	Detected	-
Aluminium[††]	-	Detected	Detected	-

*electro-conductive materials; **control material; [†]technical information provided by Carbomax AB, Sweden; [††]Detection of traces with Energy Dispersive X-ray spectroscopy (EDS) and Scanning Electrode Microscopy (SEM).

Table 2. Wastewater characteristics of the operative campaigns of this study.

Parameter	Units	Camp. 1	Camp. 2	Camp. 3	Camp. 4	Camp. 5	Camp. 6	Camp. 7	Camp. 8
pH	-	7.0 ± 0.1	6.9 ± 0.1	6.7 ± 0.1	6.0 ± 0.1	7.7 ± 0.1	7.4 ± 0.2	6.8 ± 0.2	7.3 ± 0.2
Cond.	mS cm^{-1}	0.7 ± 0.1	0.9 ± 0.1	0.3 ± 0.1	1.3 ± 0.7	0.6 ± 0.1	0.4 ± 0.1	0.9 ± 0.1	0.6 ± 0.1
T	ºC	21.9 ± 2.0	22.3 ± 2.6	14.5 ± 0.3	9.1 ± 1.0	21.3 ± 2.5	22.4 ± 0.3	23.0 ± 0.8	19.6 ± 3.4
DO	mg L^{-1}	0.5 ± 0.3	1.4 ± 0.9	2.7 ± 1.9	0.9 ± 0.1	0.2 ± 0.1	0.5 ± 0.2	0.5 ± 0.3	4.3 ± 2.9
*Eh	mV	-66 ± 40	-18 ± 66	58 ± 16	42 ± 2	139 ± 73	-10 ± 18	-7 ± 6	197 ± 151
COD	mg L^{-1}	667 ± 23	607 ± 25	398 ± 37	886 ± 49	745 ± 97	732 ± 18	381 ± 11	410 ± 79
BOD_5	mg L^{-1}	500	360	390	750	160	220	220	120
NH_4-N	mg L^{-1}	58 ± 6	49 ± 1	13 ± 2	13 ± 1	71 ± 7	24 ± 1	25 ± 1	19 ± 1
NO_3-N	mg L^{-1}	0.04 ± 0.04	0.02 ± 0.01	0.05 ± 0.04	0.03 ± 0.03	0.23 ± 0.19	0.05 ± 0.02	1.71 ± 0.54	2.35 ± 0.31
TN	mg L^{-1}	72 ± 9	49 ± 6	21 ± 10	34 ± 9	88 ± 11	37 ± 3	32 ± 9	23 ± 1
PO_4-P	mg L^{-1}	12 ± 3	8 ± 1	4 ± 1	3 ± 1	7.2 ± 1.6	1.3 ± 0.4	1.3 ± 0.2	0.7 ± 0.2
HLR	L m^{-2} d^{-1}	25	50	152	189	189	50	152	25

* ORP value vs Standard Hydrogen Electron (corrected with 207 mV at 25ºC); Camp. = sampling campaign

Table 3. Two-way ANOVA of removal rates of organic matter, nutrients and total suspended solids, based on the interaction of tested systems and HLR.

	BOD_5	COD	NH_4-N	TN	PO_4-P	TSS
R^2	0.85	0.80	0.92	0.88	0.90	0.76
F	41.47	7.13	18.45	12.15	15.94	8.37
Pr > F	< 0.0001	< 0.0001	< 0.0001	< 0.0001	< 0.0001	< 0.0001
System	2.68	24.16	16.21	14.11	163.91	13.28
	0.0215	< 0.0001	< 0.0001	< 0.0001	< 0.0001	< 0.0001
Load in	256.51	33.49	99.47	59.18	31.35	37.26
	< 0.0001	< 0.0001	< 0.0001	< 0.0001	< 0.0001	< 0.0001
System*Load in	3.43	0.77	2.35	2.08	6.54	1.79
	< 0.0001	0.94	< 0.0001	< 0.0001	< 0.0001	0.00

Table 4. Tukey HSD least square means of mass removal rates (%) of organic matter, nutrients and total suspended solids. Results classified alphabetically by tested systems. Superscript letters indicate significant differences among systems.

System	BOD_5(%)	COD(%)	NH_4-N(%)	TN(%)	PO_4-P(%)	TSS(%)
Sand/NP	85.1 ^{a}	81.6 ^{c}	40.0 ^{bc}	50.6 ^{a}	69.7 ^{b}	79.5 ^{c}
Sand/P	87.4 ^{a}	81.1 ^{c}	45.2 ^{ab}	51.0 ^{a}	72.0 ^{b}	80.3 ^{c}
PK-A/NP	87.8 ^{a}	90.6 ^{a}	35.0 ^{cd}	42.7 ^{b}	81.3 ^{a}	82.0 ^{bc}
PK-A/P	85.5 ^{a}	89.9 ^{a}	45.9 ^{ab}	51.7 ^{a}	86.9 ^{a}	80.1 ^{c}
PK-LSN/NP	87.6 ^{a}	85.9 ^{b}	33.4 ^{d}	42.9 ^{b}	40.7 ^{d}	85.7 ^{ab}
PK-LSN/P	86.9 ^{a}	86.5 ^{b}	46.4 ^{a}	51.2 ^{a}	49.0 ^{c}	89.6 ^{a}
Pr > F	> 0.05	< 0.0001	< 0.0001	< 0.0001	< 0.0001	< 0.0001
Significant	No	Yes	Yes	Yes	Yes	Yes

Table 5. Average first-order area-based removal rate constant (*k*), and correlation coefficient (R^2) for organic matter, nutrients and TSS at HLR = 55 m y^{-1}.

Material	Constant	BOD_5	COD	NH_4-N	TN	PO_4-P	TSS
PK-A/P	κ (m y^{-1})	136	128	42	24	146	133
	R^2	0.67	0.72	0.91	0.90	0.98	0.99
PK-A/NP	κ (m y^{-1})	143	139	30	14	131	128
	R^2	0.65	0.52	0.52	0.48	0.98	0.97
PK-LSN/P	κ (m y^{-1})	167	112	52	29	64	173
	R^2	0.68	0.85	0.91	0.96	0.55	0.97
PK-LSN/NP	κ (m y^{-1})	146	104	30	23	48	145
	R^2	0.71	0.86	0.53	0.97	0.37	0.97